THE INFRARED ABSORPTION SPECTRUM OF PORTLANDITE [$Ca(OH)_2$]

THE INFRARED ABSORPTION SPECTRUM OF PORTLANDITE [$Ca(OH)_2$]

By

JOHN B. WOELFLE, B.Sc.

A Thesis

Submitted to the Department of Physics

in Partial Fulfilment of the Requirements

for the Degree

Master of Science

McMaster University

September, 1958

MASTER OF SCIENCE (1958) McMASTER UNIVERSITY
Hamilton, Ontario

TITLE: The Infrared Absorption Spectrum of Portlandite [$Ca(OH)_2$]

AUTHOR: John B. Woelfle, B.Sc. (McMaster University)

SUPERVISOR: Dr. H. E. Petch

NUMBER OF PAGES: v, 53

SCOPE AND CONTENTS: The infrared absorption of a single crystal of portlandite, over a temperature range from room temperature to below the melting point of hydrogen, was studied with both polarized and unpolarized radiation. The apparatus and experimental techniques are described, and the results and their significance in relation to earlier experimental work on the crystal structure of portlandite are discussed.

Acknowledgements

The author wishes to express his sincere thanks to Dr. H. E. Petch for suggesting the problem, and for his encouragement and helpful advice during the course of the research and the preparation of this thesis.

Much of the low temperature work was performed at the McLennan Laboratory, University of Toronto, and the author is greatly indebted to Dr. E.J. Allin for making this work possible, and to Dr. W.F.J. Hare, who set up the apparatus and assisted with the experiment.

The Ontario Research Foundation, by its financial assistance, enabled the author to continue his studies and carry out this research.

TABLE OF CONTENTS

LIST OF FIGURES

CHAPTER I

INTRODUCTION

1.1 General Description of Portlandite

The first reliable physical data on crystalline calcium hydroxide were obtained with crystals which had been formed as the product of a hydration process in Portland cement. Naturally occurring crystals were first discovered at Scawt Hill, County Antrim, Ireland, by Tilley (1), who proposed the name Portlandite for the new mineral. These natural crystals were in the form of small hexagonal plates intimately associated with afwillite and calcite in larnite-spurrite contact rocks, having been ultimately derived from the hydration of the rocks.

Good artificial crystals were prepared by Ashton and Wilson (2) by the slow interdiffusion of $CaCl_2$ and NaOH solutions; they obtained hexagonal plates and prisms, the longer prisms generally having smaller cross sections at one end than at the other. With these crystals, Ashton and Wilson made accurate determinations of some of the physical and optical properties of $Ca(OH)_2$. They also reported that good $Ca(OH)_2$ crystals in the form of hexagonal plates can be produced by the action of 20 to 30 percent KOH solutions on precipitated $CaCO_3$, and that very good crystals, usually thin but up to 1 mm in diameter, have been found on the surfaces and in the interior of old cement briquettes which have been stored under water and out of contact with CO_2.

Portlandite crystals are clear and colourless, with perfect cleavage parallel to the (0001) plane. The material is very soft, and its specific gravity is 2.230 ± 0.003. The crystal is uniaxial negative, with the optic axis perpendicular to the cleavage planes. There is only moderate birefringence, the refractive indices being $n_\epsilon = 1.574$ and $n_\omega = 1.547$. Portlandite is fairly stable in dry air and only slowly dissolved by water, but when exposed to moist air or to water containing CO_2 it becomes covered in a short time with a crust of $CaCO_3$.

1.2 The Crystal Structure

The crystal structure of portlandite, which has been known for many years from X-ray diffraction studies, is of the CdI_2 layer type. It is trigonal on a hexagonal lattice with a single formula-unit per cell, and the space group is P3m1. The unit cell dimensions (3) are:

$$c = 4.895 \pm 0.003 \text{ Å}$$

$$a = 3.585 \pm 0.001 \text{ Å}.$$

The structure is shown diagrammatically in Fig. 1. Notice in Fig. 1 (a), which is a projection of portlandite on (0001), that all the ions are in special positions on triad axes which run parallel to the crystallographic c axis. Each calcium ion is located at the centre of an octahedron formed by the six nearest hydroxyl ions, and the octahedra are joined together in sheets by having hydroxyl ions in common. Each sheet consists of three parallel layers of ions, the calcium ions lying in a single plane which is sandwiched between two layers of hydroxyl ions. The sheets are piled vertically upon each other in the crystal. Strong electrostatic forces hold together the ions within a given sheet, while

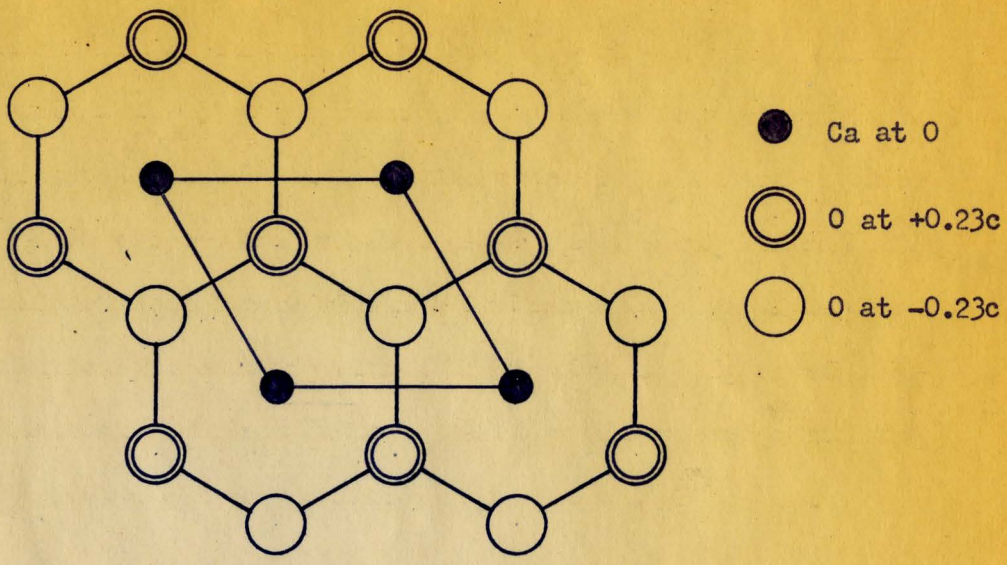

(a) Structure of Portlandite Projected on (0001)

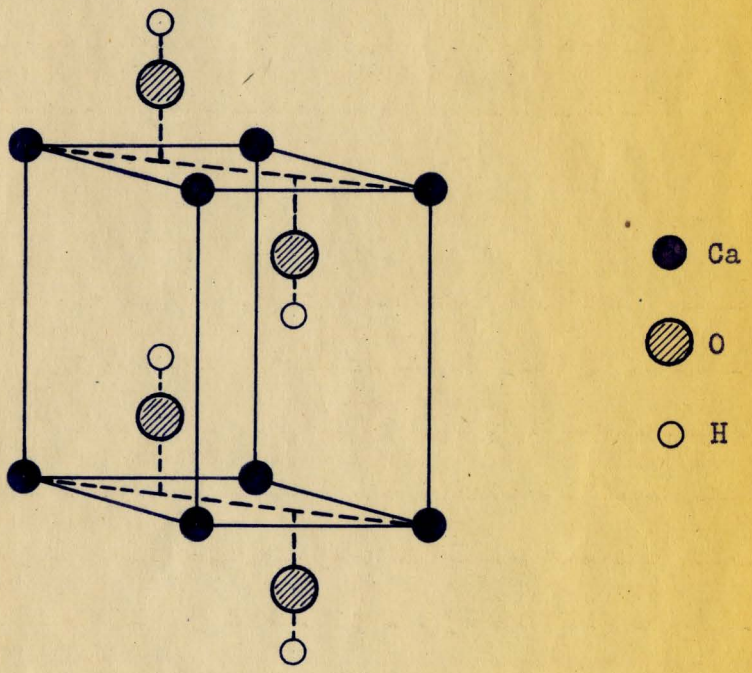

(b) Structure of Portlandite Showing One Unit Cell of the Hexagonal Lattice

Fig. 1. The Crystal Structure of Portlandite

only weak van der Waals forces act between sheets, thus accounting for the easy cleavage between them.

1.3 Previous Experimental Work

The mineral brucite, $Mg(OH)_2$, is isomorphous with portlandite. Accordingly, the general properties connected with the structure can be expected to be nearly identical for the two crystals; the slight differences arise only from the fact that in brucite magnesium ions take the place of the calcium ions in portlandite. Because such general properties are of concern here, it is advantageous to discuss experimental work on both brucite and portlandite.

The structure for brucite was worked out almost forty years ago by Aminoff (4), using X-ray techniques. In the early thirties, Megaw (3) used X-ray methods to obtain accurate values for the unit cell dimensions and oxygen positions for portlandite and brucite. It was not possible at that time to locate the hydrogen atoms by direct methods, but Bernal and Megaw (5), on the basis of symmetry and electrostatic considerations, proposed that the O-H bonds are parallel to the c axis [see Fig. 1 (b), which shows one unit cell with the predicted hydrogen positions]. Bernal and Megaw ruled out the possibility of hydrogen bonding between layers because of the large distance (about 3.3 Å) between nearest oxygen atoms in adjacent sheets.

Recently, Mara and Sutherland (6) made a detailed study of the infrared absorption spectrum of brucite in the OH - stretching region, and found the spectrum to be very complex between 2μ and 3.5μ (5000 and 2850 cm^{-1}). On the basis of the Bernal-Megaw model for the brucite

structure, it was thought that there should be only one OH-stretching band near 2.75μ. With only two hydroxyl ions in the unit cell, the OH normal modes of the cell would consist of only the in-phase and the out-of-phase vibrations. The first gives no net change in the dipole moment and is therefore infrared inactive; hence there is only one infrared-active OH vibration frequency. This band should show complete polarization, with the change in dipole moment parallel to the c axis. Mara and Sutherland found such a band, but observed in its immediate neighbourhood at least 15 other bands which exhibited a variety of polarization properties. Examining the spectrum of $Mg(OD)_2$, they found the complex pattern of bands to be shifted by a constact factor (nearly $\sqrt{2}$) to longer wavelengths. They concluded that most of these bands must represent true OH-stretching fundamentals, not combinations with low lattice frequencies involving the magnesium ions, and hence that the unit cell must be much larger than deducted from X-ray analyses. Moreover, they concluded that the polarization properties of the bands proved that Bernal and Megaw's prediction of the hydrogen positions was incorrect. They also felt that they had demonstrated the much greater sensitivity of the infrared method, compared to the x-ray method, in deciding about the positions of hydrogen atoms in crystals. Because portlandite has the same crystal structure as brucite, the conclusions of Mara and Sutherland should apply to it as well.

Petch and Megaw (7) undertook a re-examination of brucite and portlandite by X-ray methods. No evidence was found for a larger unit cell in either crystal, and the accepted unit cell dimensions and space group were confirmed. Petch and Megaw argued further, mainly on the

basis of symmetry and electron-bonding effects, that the hydrogen positions proposed by Bernal and Megaw were correct, although the possibility of statistically disordered displacements of the hydrogen atoms was not ruled out. Petch also made a preliminary examination of the infrared absorption in portlandite, and obtained a complex spectrum similar to that found in brucite by Mara and Sutherland. The apparent discrepancy in the results obtained by infrared methods and by modern X-ray techniques stimulated a new interest in the structures of portlandite and brucite.

More recently, Petch (8) reported that a study of portlandite using a Geiger counter X-ray diffractometer and the technique of the $(F_o - F_c)$-synthesis gave strong evidence supporting Bernal and Megaw's prediction for the hydrogen positions. In addition, Elleman and Williams (9) located the protons in brucite by nuclear magnetic resonance. Their data also support the Bernal-Megaw model.

In the light of this X-ray and nuclear magnetic resonance work, Mara and Sutherland (10) carried out some further infrared work on brucite. They examined the spectrum at the temperature of liquid nitrogen, and found that many of the low frequency bands disappeared. They were forced to conclude, in contradiction to their earlier convictions, that these bands are combination difference frequencies arising from energy levels due to an exceptionally low OH-deformation mode, and that the spectrum can be explained, in principle at least, without invoking a larger unit cell or changing the equilibrium positions of the hydrogen atoms from those proposed by Bernal and Megaw. They also mentioned a suggestion by Hexter, later reported by Hexter and Dows (11), that a low frequency "libration" of the OH ion may combine with

the vibration to produce the complex infrared spectra of brucite and portlandite. Mara and Sutherland felt that their observations at low temperature confirmed this suggestion, although the full explanation of the fine structure still presented many difficulties.

Thus, many questions about the behaviour of the layer-type structures of portlandite and brucite remained to be answered. A full study of the infrared absorption of portlandite was required in order to ascertain how closely the spectrum corresponds with that of brucite. A detailed examination of the temperature effects was desirable, in the hope of gaining a better understanding of infrared absorption in solids, and, in particular, of the mechanisms leading to the complexity of the infrared spectra of brucite and portlandite. Because of the unexplained discrepancy between X-ray and infrared results, the value of infrared techniques as an aid in locating hydrogen positions was open to serious doubt, and further work was required to settle this question. With these considerations in mind, the present work was undertaken.

CHAPTER II

EXPERIMENTAL APPARATUS AND TECHNIQUES

2.1 The Samples

The portlandite samples were obtained from a large single crystal which was prepared by the hydration of larnite (Ca_2SiO_4) by Professor C. E. Tilley, Department of Mineralogy and Petrology, Cambridge University. The original crystal was in the form of a hexagonal prism with the approximate dimensions 3.5 mm x 3.5 mm x 7 mm. From it Dr. H. E. Petch cleaved several plates about 50 microns thick for infrared work, and also prepared samples which he used for X-ray analyses (7, 8, 12). Powdered samples for the infrared work were made from some of the remaining fragments.

Because the individual crystal plates did not have a sufficiently large cross-sectional area, a composite section was made up of three plates. They were from the same part of the original crystal; two of them were complete hexagons, and the other was a large portion of a hexagon. The original crystal had a slight ridge along one of the edges and the resultant projection at one corner of each thin section made it easy to arrange them so that they had the same orientation, as shown in Fig. 2. The composite section was mounted over a slit as indicated in the figure. Since the crystals were placed very close together, the amount of radiation which could pass between them was negligible. These three plates were used for all the room temperature work.

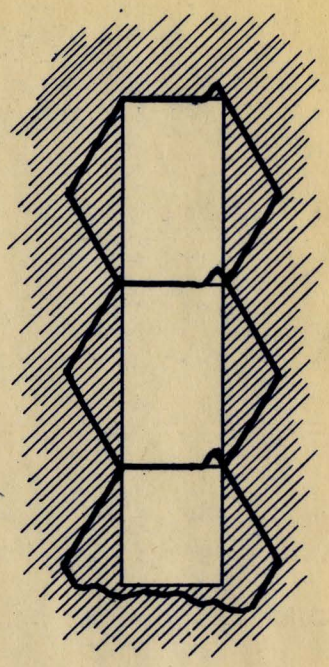

Fig. 2. Alignment of the Portlandite Crystal Plates in the Composite Section

Early in the course of the low temperature work, the three pieces became covered with a white crust which rendered them almost opaque to visible and infrared radiation. A leak had developed in the vacuum chamber in which the crystals were mounted. Possibly water vapour entered the chamber and solidified on the crystals, and later reacted with them when they returned to room temperature.

Most of the opaque layer was removed by rubbing the surfaces of the crystal plates with a small camel-hair brush moistened in a paste of jeweller's "white rouge" and hexachlorobutadiene. The crystals were restored almost to their original condition except for somewhat reduced transparency. This reduction was caused by an increase in scattering due to the irregularities left on the surfaces of the plates as a result of the reaction and subsequent polishing process. A check of the infrared spectrum at room temperature and at liquid air temperature indicated that the absorption properties were unchanged.

One of the pieces used in the room temperature work, the partial hexagon, was broken in the process of polishing. It was replaced in the composite section by a plate obtained from a different part of the original crystal. This plate was a complete hexagon, but had a hole near the centre through which radiation could pass. The hole was small, however, and the increase in transmission was not appreciable.

The powdered samples were prepared by grinding fragments of portlandite with a small mortar and pestle, and mulling in hexachlorobutadiene or nujol. Hexachlorobutadiene is especially well suited to the purpose, for it is almost transparent in the most interesting part of the portlandite spectrum: from 5000 to 3200 cm $^{-1}$ it has no absorption bands, and

from 3200 to 2800 cm $^{-1}$ it has only a few weak bands.

Thin sections of brucite were cleaved from a large, flaky sample found in Lancaster County, Pennsylvania, for which the author wishes to thank Dr. D. M. Shaw, Department of Geology, McMaster University. The sections were approximately 60 microns thick, although not so uniform in thickness as the portlandite plates. As in the case of portlandite, a composite section was prepared using three pieces of brucite mounted side by side in the same plane. Accordingly, the c axes of the pieces were parallel, because the c axis is perpendicular to the cleavage planes in brucite, as in portlandite. The three pieces were irregular in shape, and no attempt was made to orient them with corresponding a axes parallel.

2.2 The Spectrometers

Most of the spectra were obtained with a Perkin-Elmer Model 21 Infrared Spectrophotometer equipped with a 60° CaF_2 prism. It is a double-beam, recording spectrometer with a thermocouple detector and a Nernst glower source. Percent transmission is recorded as a function of wavenumber; both scales are linear. The wavenumber scale was calibrated by using atmospheric absorption bands as standards, as well as some methane and ammonia bands. The spectral range with the CaF_2 prism is 9000 to 1200 cm^{-1}.

For the spectra obtained in the McLennan Laboratory, University of Toronto, a Perkin-Elmer Model 12C Infrared Spectrometer with a 60° LiF prism and a thermocouple detector was employed. The infrared source was a water-cooled globar, and the beam was focused first on the sample and then on the spectrometer slits by means of two rock salt lenses.

The spectrometer was connected to a continuous-chart recorder which gave a plot of transmission vs. wavenumber. The latter scale was not linear; a chart, prepared in the McLennan Laboratory using atmospheric and ammonia absorption bands, was used to calibrate the spectra. The Model 12C is a single-beam instrument, and hence it was necessary to enclose the entire optical system and flush it with dry nitrogen gas in order to reduce the absorption by atmospheric water vapour. Without flushing, the strong water bands between 4000 and 3500 cm^{-1} would have obscured the portlandite spectrum in that region. With the Model 12C, the spectrum of portlandite was studied in the region from 4700 to 2800 cm^{-1}.

2.3 The Crystal Mounts

The crystal holder assembly for the room temperature work is shown actual size in Fig. 3. The back plate (E) is part of the rotatable cell manufactured by Perkin-Elmer for use with their instruments, and is machined steel. It fits into a cell holder in either beam of the spectrometer. The other parts were made of brass. The crystal holder fits down through the holes in the two brackets (F), which are fastened to the back plates with Allen screws (G). The holder was machined to rotate freely, and the assembly was mounted on the spectrometer with the axis of rotation of the holder vertical. A reference line (H) was cut into the top bracket, and the calibration marks (A) placed at 30 intervals on the holder as shown. The sides of the slit (B) which is about 2mm x 10 mm in size, are knife-edged, the brass having been filed away at the back so that the holder can be rotated $\pm 60^{\circ}$ without part of the beam through the sample being cut off by the edges of the slit. The crystal plates were

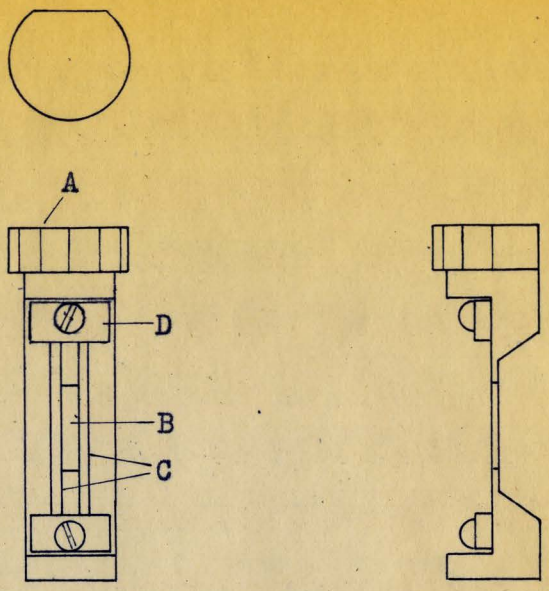

(a) Crystal Holder (A, Calibration Marks; B, Slit; C, Pieces of Watch Mainspring; D, Brass Block)

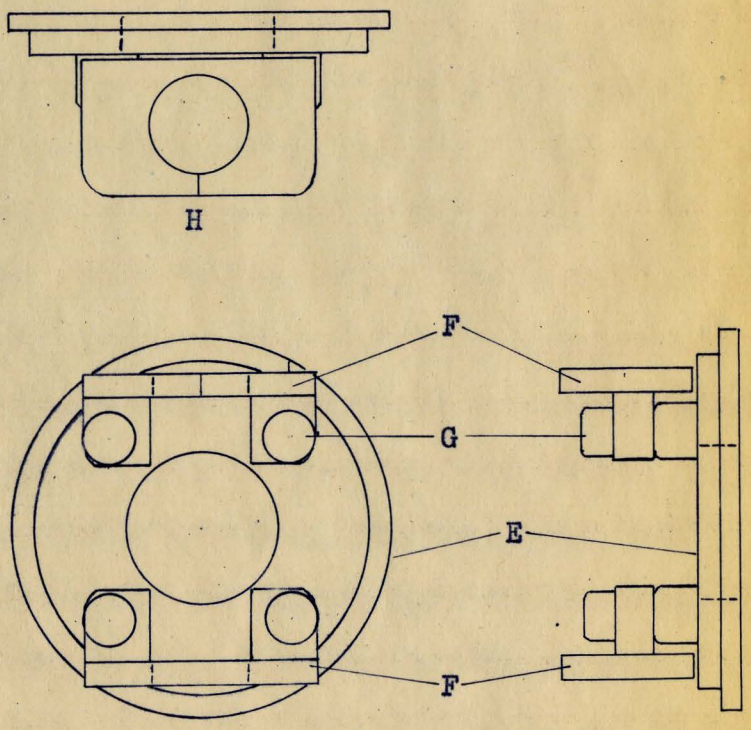

(b) Holder Frame (E, Back Plate; F, Brackets; G, Allen Screws; H, Reference Line)

Fig. 3. Crystal Mount for Room Temperature Work

mounted by having two corners held against the flat face of the crystal holder by pieces of watch mainspring (C). The spring strips were clamped at both ends by two small brass blocks (D), which had shallow grooves cut in the back to hold the springs in position along each side of the slit.

Full-scale views of the low temperature cell used with the Model 21 spectrometer appear in Fig. 4. The cell was designed with assistance from Mr. T.H. Bryden, and constructed of brass in the machine shop, McMaster University. Except for the permanent join at the top, the inner part (A) of the cell is completely isolated from the outer walls by B, a chamber which is evacuated when the cell is in use. The rubber O-ring (C) shown in the cross-sectional view provides a vacuum seal between the two main parts of the cell, which are held together by four machine screws as shown. Two openings (D) were placed in the lower part to permit the spectrometer beam to pass through, and CaF_2 windows of dimensions 22.5 mm x 9.5 mm x 1 mm were fastened over them with Armstrong cement. E, the back plate, was designed to fit into the cell holders of the spectrometer; with it the assembled cell was held securely enough that no further support was needed. The crystal holder (F), which is not shown in the front view, is similar in design to the one previously described, with the crystals held in place over a slit by flat pieces of spring. It was found that the lower spring clamp had to be left slightly loose to allow for the different expansion coefficients of brass and steel. The spring strips contracted less than the brass holder upon cooling, and if clamped tightly at both ends, they buckled outward and

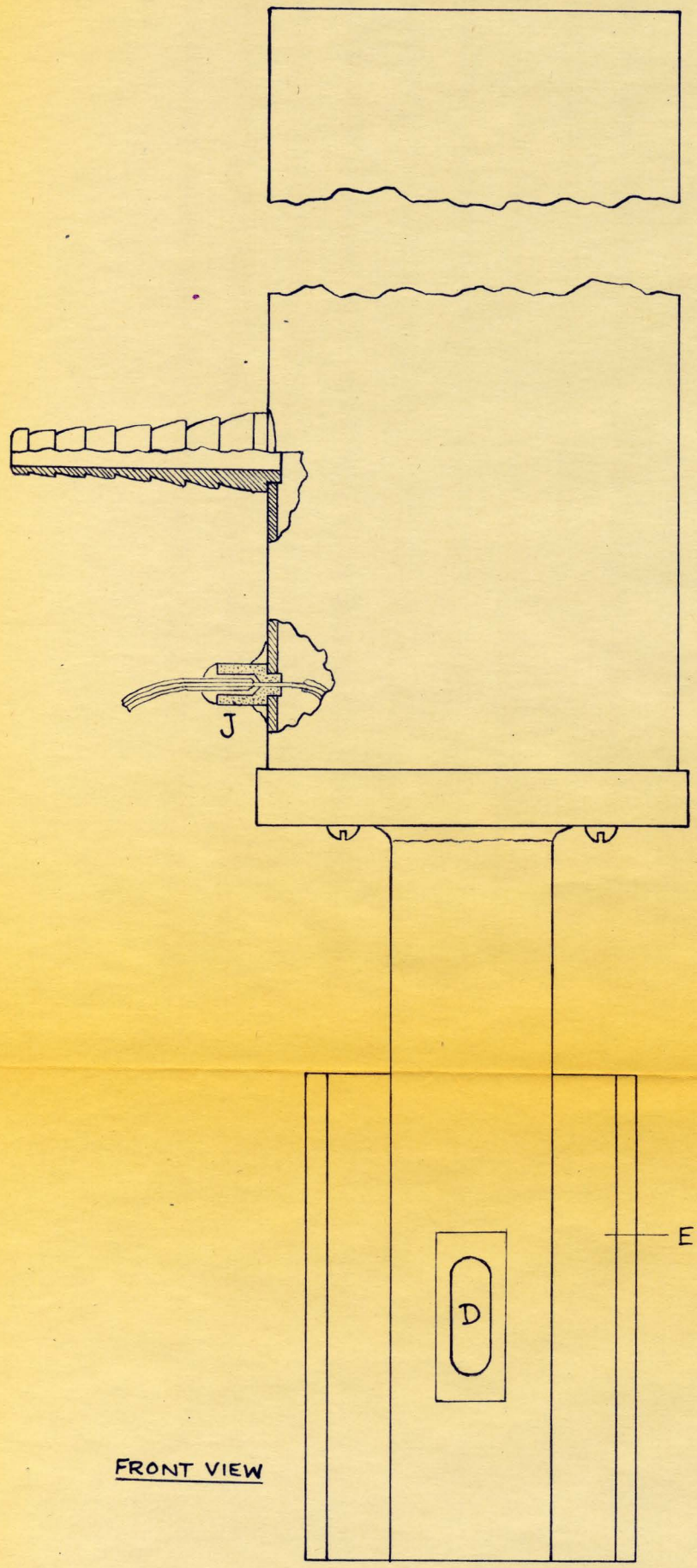

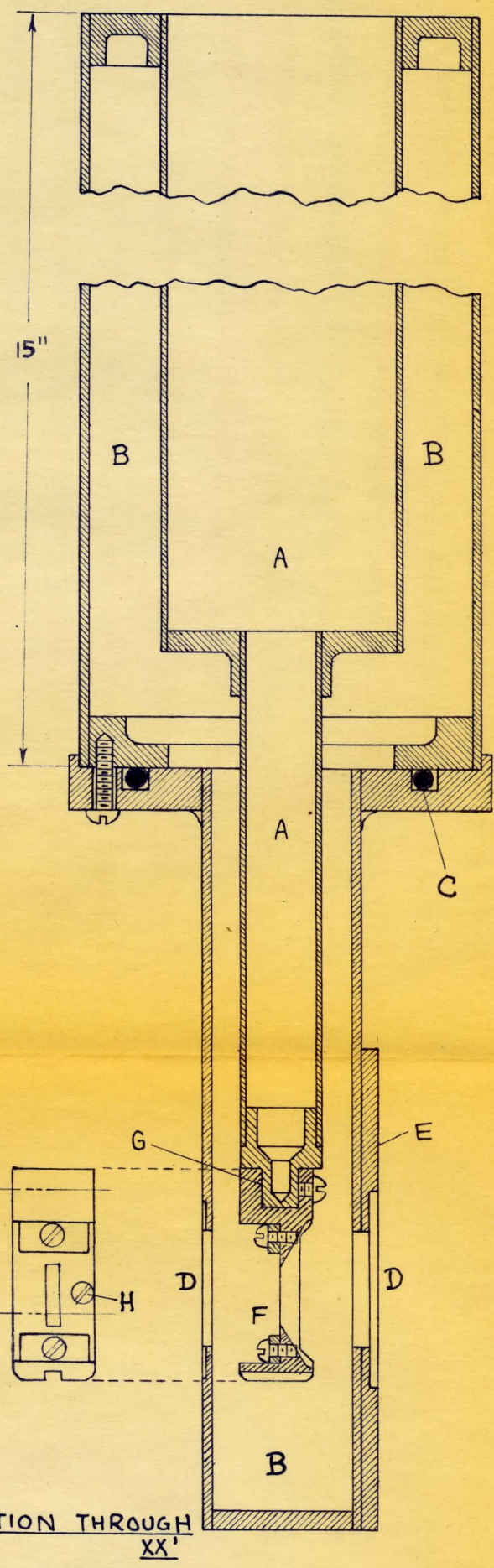

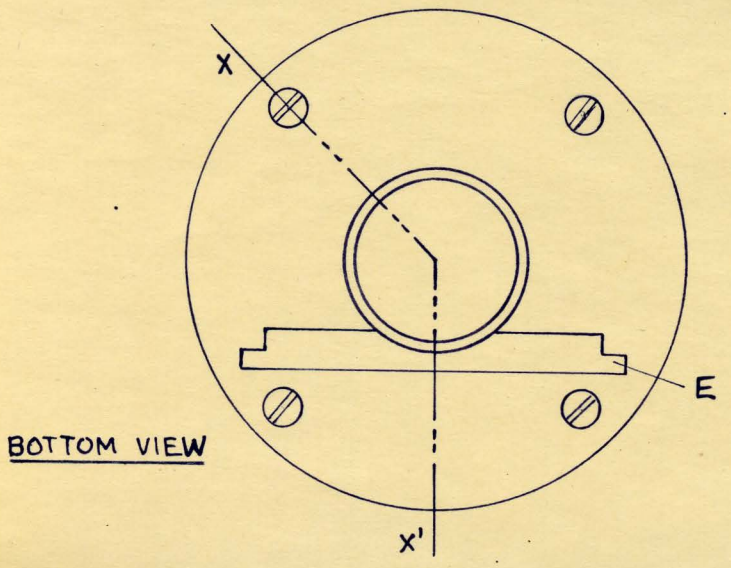

Fig. 4. Low Temperature Cell Used with the Model 21 Spectrometer (A, Inner Cell ; B, Vacuum Chamber ; C, Rubber O-ring; D, Windows for Spectrometer Beam ; E, Back Plate ; F, Crystal Holder ; G, Pivot Stud; H, Brass Machine Screw ; J, Plastic Insulator

and permitted the crystals to slip out of position. The holder pivots on the stud (G), but fits snugly enough to provide good thermal contact between the two parts; it is held firmly in place by means of a small set screw. The flat portion of this holder is thicker than that of the room temperature holder in order to provide increased heat conduction. Enough brass was removed from behind the slit to permit the holder to be rotated ±40° without the back edges cutting off part of the beam.

A copper-constantan thermocouple was fastened to the holder by means of a small, brass machine screw (H), and the two leads were brought out through lucite insulators, one of which, J, is shown in the front view; Armstrong cement was used to fasten the wires and insulators in place and to provide the vacuum seal. After chamber B had been evacuated, a coolant such as liquid air was poured into A, thereby cooling the brass holder and mounted crystals. Tests were made with the thermocouple placed in three different positions over the length of the slit, and the temperature gradient was found to be negligible. Temperature measurements during the course of the infrared work were taken with the thermocouple fastened in the central position.

For temperatures down to about 4°K, the crystals were mounted in a liquid helium cryostat. The cell and holder for the purpose are shown in Fig. 5. The cell (A) was made of pyrex glass, and sapphire windows (B), 1¼ inches in diameter by 1 mm thick, were fastened in place with araldite cement. The crystal holder (C), similar to the other two in principle, is soldered to C, a ¼-inch monel tube. The spring strips are not shown. The tube and holder were kept central in the glass tube by two lucite bush-

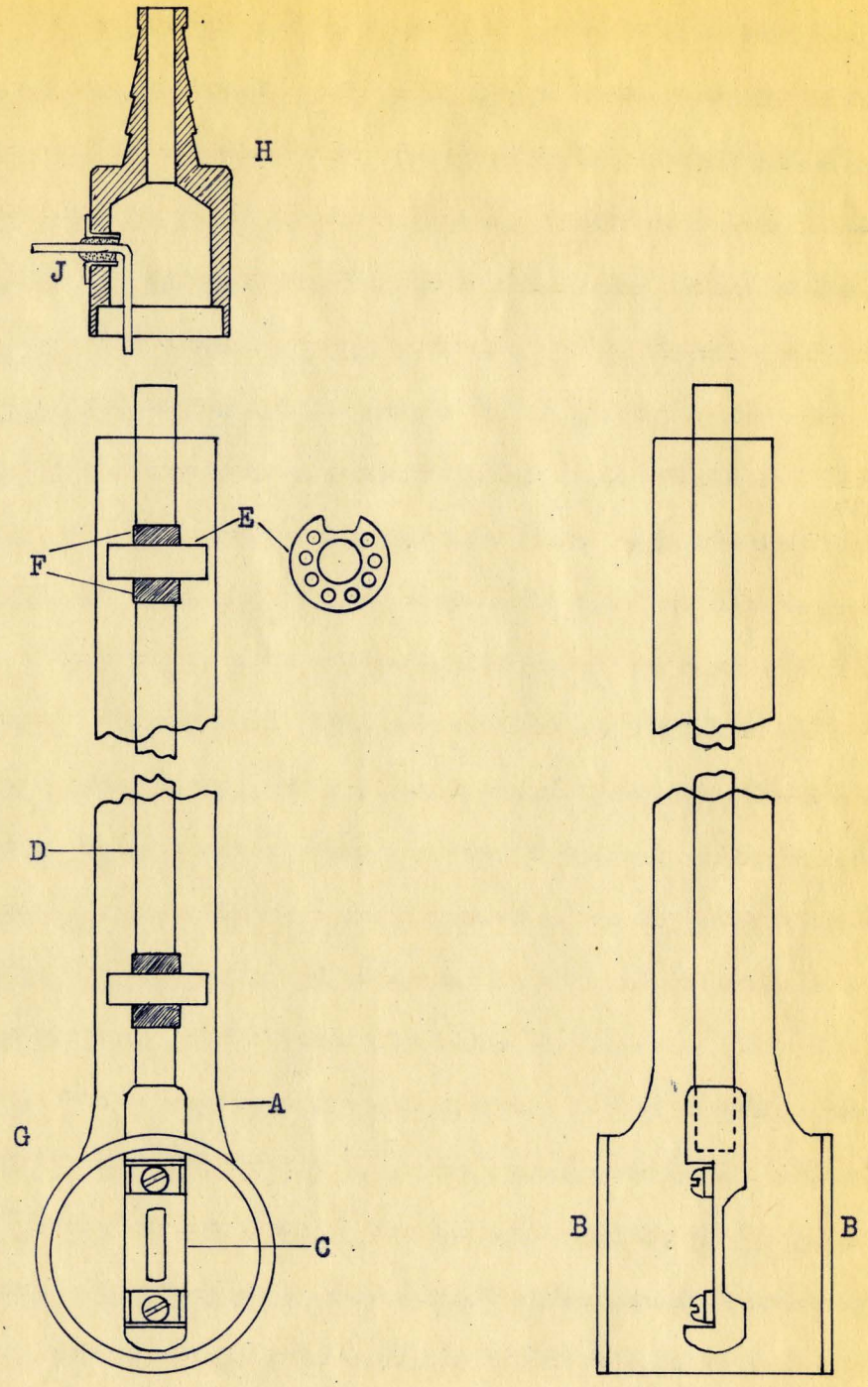

Fig. 5. Cell and Crystal Holder for the Liquid Helium Work (A, Pyrex Cell; B, Sapphire Windows; C, Crystal Holder; D, Monel Tube; E, Lucite Bushing; F, Scotch Electrical Tape; G, Brass Machine Screw; H, Brass Fitting; J, Kovar Terminal)

ings (E) of the form shown in the figure. The notch is for thermocouple leads, and the holes are to permit hydrogen gas to pass down the tube to the cell at the bottom. The bushings were each kept from sliding up or down the tube by two thin strips of Scotch electrical tape (F) wound around the tube for a couple of turns, as shown in the front view. A copper-constantan thermocouple was fastened to the crystal holder by means of G, the screw holding the top spring clamp, and the leads were brought out through H, the brass fitting (shown in cross section), by means of two kovar seals, one of which is shown (J). H was fitted over the end of the glass tube and fastened with black sealing wax, after the tube had been mounted in the brass top plate (A) of Fig. 6.

In Fig. 6, a cross-sectional view of the liquid helium cryostat is shown. The outline of the crystal cell is sketched to indicate its position in the cryostat. B is a kovar metal-to-glass seal joining the metal top to the pyrex body of the cryostat. The beam can pass through the cryostat by means of rock salt windows (C), $2\frac{1}{4}$ inches in diameter by $\frac{1}{4}$ inch thick, and sapphire windows (D), 1 inch in diameter by 1 mm thick, which are fastened in place with araldite cement. The chambers designated by E are permanently evacuated. Rubber O-rings at positions F, G, and H provide airtight seals between the various parts of the apparatus. The crystals were rotated without breaking any of the seals by loosening slightly the knurled nut (J) which exerts pressure on the O-ring at F, and then rotating the entire crystal cell through the required angle. The nut was then tightened again.

The outer dewar flask was kept filled with liquid air (K). The cryostat was pre-cooled for a few hours before liquid helium was intro-

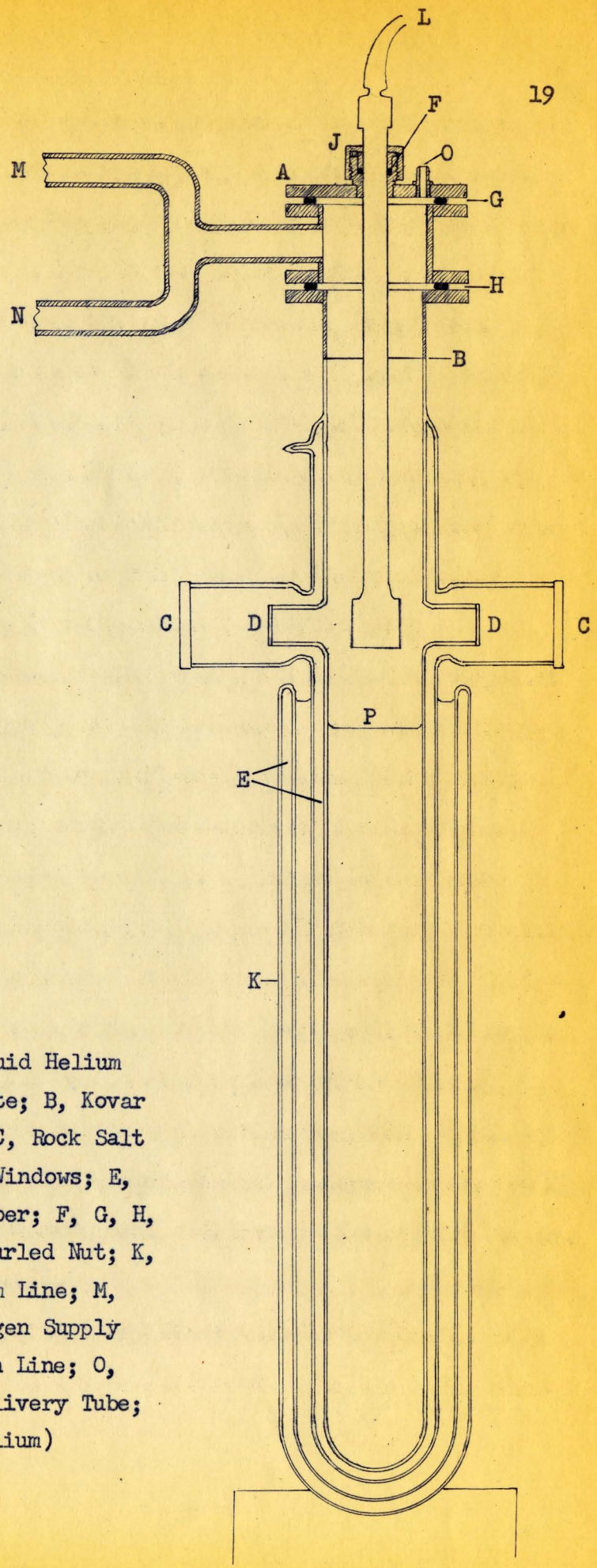

Fig. 6. The Liquid Helium Cryostat (A, Top Plate; B, Kovar Metal-to-Glass Seal; C, Rock Salt Windows; D, Sapphire Windows; E, Permanent Vacuum Chamber; F, G, H, Rubber O-Rings; J, Knurled Nut; K, Dewar Flask; L, Vacuum Line; M, Vacuum Line and Hydrogen Supply Line; N, Helium Return Line; O, Opening for Helium Delivery Tube; P, Level of Liquid Helium)

duced. To ensure that no water vapour condensed or crystallized in the system, the crystal cell and the cryostat were kept evacuated through lines L and M respectively. A few spectra were obtained during the pre-cooling period.

Before liquid helium was put into the cryostat, line L was closed and the helium return line (N) opened to permit the cryostat to fill with helium gas at atmospheric pressure. The cell was kept evacuated in order to reduce the thermal shock to the crystals when the liquid helium first entered the cryostat. The liquid helium was transferred from its container by means of a double-walled metal tube which fits through an opening (O) in the top plate and down into the bottom of the cryostat. After the cryostat had been filled to the level (P) shown in Fig. 6, the transfer tube was removed and the opening in the top plate sealed with a rubber stopper. As the helium boiled off, it returned to the liquifier through the helium return line, cooling the walls of the pyrex cell as it passed by. Several spectral runs were made as the crystals slowly cooled. To attain very low temperatures, dry hydrogen gas was introduced into the cell to improve the thermal contact between the walls of the cells and the crystals. The temperature of the cell was controlled by an electric heater which was suspended close to the bottom of the cryostat. Increasing the heater current caused the helium to boil more rapidly, and the increased flow of cold gas past the cell caused greater cooling. There were, as well, a few turns of heater wire wound around the cell in case it was necessary to raise its temperature fairly quickly. The four leads from the heaters were brought out of the cryostat by means of three kovar terminals on the top plate.

The thermocouple provided good temperature down to liquid air temperatures. Below that, as the flatter part of the emf vs. temperature curve was reached, the determinations became less accurate. At temperatures below 20°K, however, some of the hydrogen which had been introduced into the cell liquified at the bottom, and the temperature was determined accurately by measuring the hydrogen vapour pressure (13). The runs at lowest temperature were made with hydrogen solidified at the bottom of the cell; the amount in the cell was adjusted until the crystal holder was immersed in solid hydrogen to a level just below that of the crystals, thus assuring that the crystals were at a temperature very close to that of the solid hydrogen.

2.4 Auxiliary Equipment

The polarizer, manufactured by Perkin-Elmer, consists of six 0.020-inch AgCl plates enclosed in a bakelite case, and a wedge window of NaCl to compensate for the lateral shift of the beam by the plates. The orientation of the polarizer can be varied through ±90° on a scale marked in 10° intervals. Transmission over the spectral region studied is about 30%.

For studying the mulled samples, Perkin-Elmer demountable cells were used, with two CaF_2 windows, 1 inch in diameter by 1 mm thick. The windows are held between two metal plates which are tightened together by four Allen screws. The sample is placed between the windows. Lead spacers can be used to vary the sample thickness, but good spectra were obtained without a spacer. A small amount of the mulled sample was used, and as the windows were squeezed together,

it spread out to form a layer of uniform thickness.

As mentioned earlier, the slit across which the crystal plates were mounted was only 2 mm x 10 mm. At the position in which the samples were placed, however, the beam dimensions of the Model 21 spectrometer are about 6 mm x 19 mm. There is an optical balance control consisting of a comb with wedge-shaped teeth which can be moved in and out of the sample beam, but it was desirable to maintain the balance control close to the fully open position in order that most of the radiation which passed through the sample would reach the detector. It was necessary, therefore, to provide compensation in the reference beam so that the intensities of the two beams would be approximately equal. For this purpose, cardboard disks with slits of varying widths were used. For each angle at which the crystal holder was set, a compensator having a slit width approximately equal to that of the effective width of the holder slit was used. A demountable cell was employed to mount the disk in the reference beam.

A demountable cell was also used to hold a compensating cell for use with the liquid air apparatus, as illustrated in Fig. 7. The 5 mm thick CaF_2 windows (A) were placed at the ends of a short, brass cylinder (B) fitted with a hose connection so that it could be evacuated. Rubber washers (C) provided the necessary seal between the windows and the brass cylinder. The assembly was held together between the metal plates (D) of the demountable cell, using $1\frac{1}{2}$-inch screws in place of the $\frac{1}{2}$-inch Allen screws normally employed. The total path length of the evacuated compensating cell was approximately equal to that of the liquid air cell; hence atmospheric absorption remained almost equal in the two beams. A single, cardboard disk, E, was

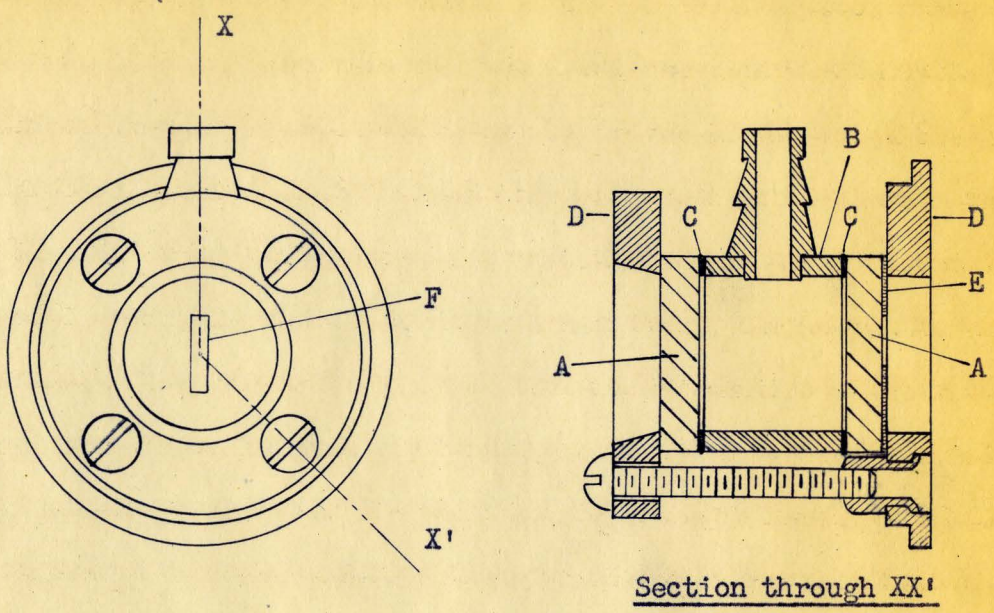

Fig. 7. Compensating Cell for Use with the Low Temperature Cell (A, CaF_2 Windows; B, Brass Chamber; C, Rubber Washers; D, Demountable Cell Plates; E, Cardboard Disk; F, Slit)

incorporated in the cell. The width of the slit (F) was varied as required simply by using masking tape.

The thermocouples used with the low temperature apparatus were made of a single strand of #23 copper wire and a few strands of #28 constantan wire (two in the case of the liquid air cell, and three in the case of the liquid helium holder) twisted together. The effect of inhomogeneities in the constantan wire is partially cancelled by the use of more than one strand (14). The thermo-junctions were made by the electric-arc method described by Wood and Cork (15). After the ends of the copper and constantan leads had been twisted together for a few turns, the positive side of a 110-volt DC line was connected to the wires near the end. The negative terminal was connected through a resistance of about 100 ohms to a carbon rod which was mounted on a wooden handle. The rod was brought up to the end of the wires, and drawn away again as soon as the arc was formed, leaving the copper and constantan wires fused together.

In the case of the liquid air cell, the constantan lead from the junction on the crystal holder was brought out through the jacket of the cell to the reference junction without interruption. The reference junction was enclosed in a glass tube which was submerged in ice water. The copper leads from the two junctions were connected to the potentiometer. "Spaghetti" insulation was used on the leads wherever necessary to ensure that they did not come into contact with each other or with other metal parts.

The leads of the thermocouple used with the liquid helium apparatus were not brought out of the cell without interruption, kovar terminals having been used as described earlier. Since the top of the glass

tube and the brass fitting remained at room temperature throughout the experiment, the thermal gradient across each terminal was probably negligible. It is unlikely, therefore, that any appreciable error in the temperature determination was introduced by the interruptions in the leads. As with the liquid air apparatus, the reference junction was immersed in ice water, and insulation was used on the leads where necessary.

The potentiometer was a Leeds and Northrup Type K, which is a slide-wire type. A 1.0183 volt standard cell was used, and a Griffin and Tatlock moving-coil galvanometer having a sensitivity of 0.9 microvolts per mm scale division.

The thermocouples were calibrated by obtaining the thermal emf at three fixed points: the melting point of mercury (-38.9°C), the melting point of ether (-116.3C), and the boiling point of oxygen (-183.0°C). With these three points a calibration curve of thermal emf vs. temperature was drawn, using as a guide a curve plotted from typical emf vs. temperature values given by Scott (16). Down to -190°C, temperature values, were estimated to be accurate within about 1°C. Below that temperature, the necessary extrapolation combined with the flattening of the curve resulted in rapidly decreasing accuracy.

CHAPTER III

EXPERIMENTAL RESULTS AND DISCUSSION

3.1 Spectra Obtained at Room Temperature with Unpolarized Radiation

The spectrum (for the range 4100-2800 cm^{-1}) of portlandite powder mulled in hexachlorobutadiene is shown in Fig. 8; the dominant feature is a very intense absorption band centred at 3650 cm^{-1}. The ordinate for this and most of the following spectra is percent transmission. The scale is linear, but recorded values of transmission vary considerably with operating conditions, making it difficult to assign absolute values. The vertical axis, therefore, is not calibrated. Although there may be some reflection by the sample, it is assumed that decreases in transmission are due principally to absorption, and that the peaks appearing in the spectra are absorption bands.

For all further work on portlandite, the composite section of thin plates was used. Fig. 9 shows how the spectrum (over the range 4100-3100 cm^{-1}) changes as φ, the angle between the crystallographic c axis and the incident beam, increases. The angle φ is illustrated in Fig. 10(a). Because the intensity of radiation at the detector decreased as φ became greater (for the reason discussed on Pages 21 and 22) the absorption bands became less sharply defined. For reproducing the spectra, the intensity of absorption of the broad band in the 4000-3800 cm^{-1} region for $\varphi = 0^{\circ}$ was used as a standard, and the vertical scales of succeeding spectra expanded as necessary to give the same peak height. Although the procedure

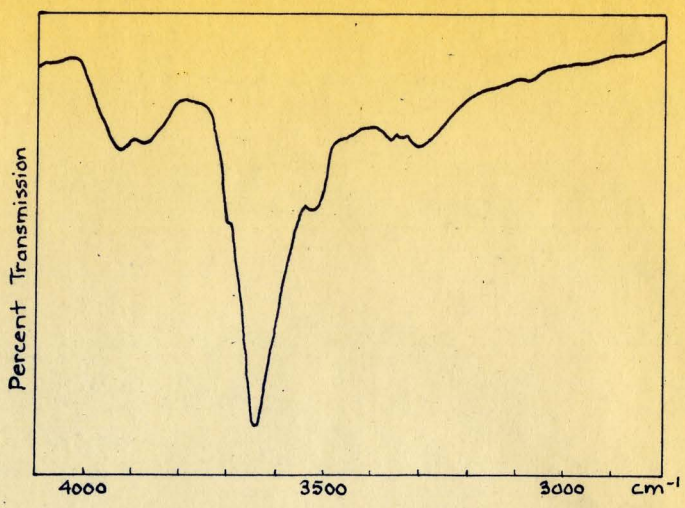

Fig. 8. Infrared Spectrum of Portlandite Powder Mulled in Hexachlorobutadiene

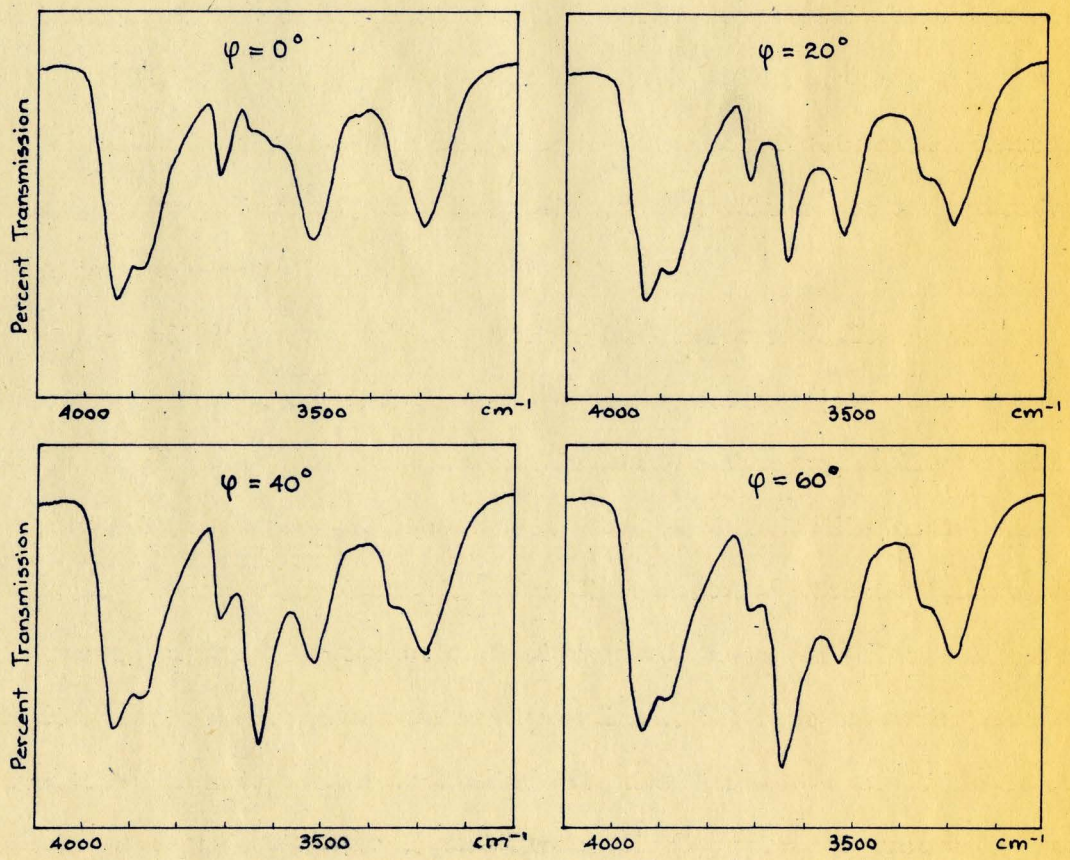

Fig. 9. Infrared Spectra of Portlandite at Room Temperature with Unpolarized Radiation and Various Orientations of the Crystallographic c axis

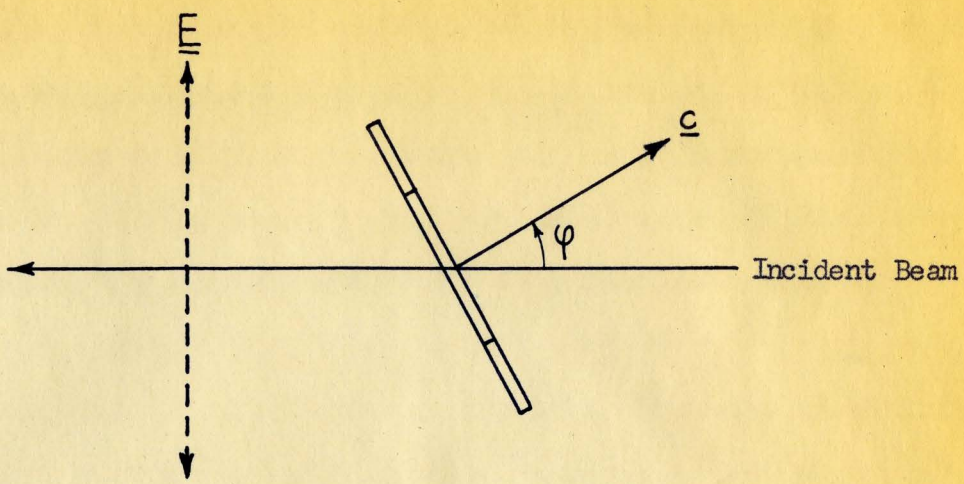

(a) Top View of the Sample

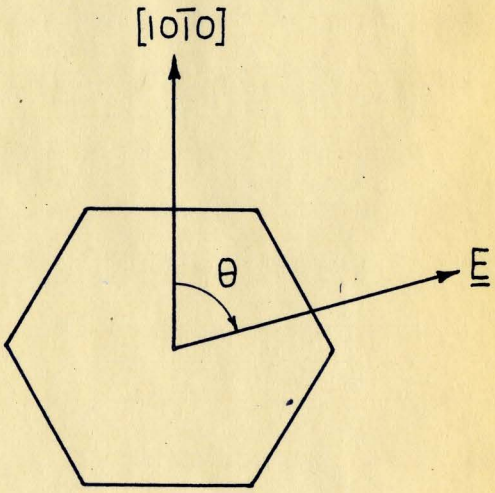

(b) View of the Sample Looking in the Direction of the Incident Radiation

Fig. 10. Orientation of the Crystallographic c Axis and of the E Vector of the Incident Radiation

may not be fully justified, later work indicated that there is little or no change in the intensity of this band over the range of orientation employed. The only apparent change in this series was in the band at 3650 cm^{-1} which had minimum intensity when φ was zero, and greatly increased in intensity as φ increased, that is, as the c axis became more nearly parallel to the plane containing the electric vibrations of the incident radiation.

The spectra of Fig. 9 indicate why the 3650 cm^{-1} band predominates in the spectrum of powdered portlandite. From the great increase in the intensity of this band as φ increases, it appears that when the optimum orientation for this band is reached ($\varphi = 90°$), its intensity will be much greater than that of the other bands in this part of the spectrum. In other words, if the c axis were perpendicular to the direction of the incident radiation, the 3650 cm^{-1} band would be much more intense than the others. In a powdered sample containing many small particles of portlandite with random orientation of the c axis, therefore, it could be expected that the 3650 cm^{-1} band would be quite strong, as Fig. 8 shows.

Since the object of the above study was to ascertain the general character of the spectrum at room temperature, the spectrometer was operated with low resolution in order to permit a higher scanning speed. All further work was done with high resolutions. Most of the experimental work was done with the Model 21 spectrometer equipped with a CaF_2 prism; hence the spectroscopic equipment will not usually be mentioned except for the spectra obtained with the other equipment.

3.2 Spectra Obtained at Room Temperature with Polarized Radiation

The absorption spectrum for polarized radiation was studied with

and 40°.

crystal orientations of $\varphi = 0°$, 20°, At each of these orientations the $\underline{E}$ vector was rotated, and the spectrum observed with $\Theta = 0°$, 30°, 60°, 90°, 120°, and 150°, where Θ is the angle between the $[10\bar{1}0]$ direction and the $\underline{E}$ vector. The angle Θ is illustrated in Fig. 10 (b).

This study strikingly demonstrated the complete polarization of the 3650 cm^{-1} band, but revealed no further polarization properties in the spectrum of portlandite at room temperature over the frequency range studied. Some of the spectra, from 4100 to 3000 cm^{-1}, are shown in Fig. 11. For this series, φ was constant at 20°, while Θ was 0°, 30°, 60°, and 90° in turn. In reproducing these spectra, some adjustment was made for an overall change in transmission which occurred when the orientation of the polarizer was varied. In this series the band at 3650 cm^{-1} appears, with its intensity increasing as Θ increases until it reaches a maximum when $\Theta = 90°$. When $\Theta = 90°$, $\underline{E}$ lies in the plane defined by the $\underline{c}$ axis and the incident beam; the component of $\underline{E}$ in the direction of $\underline{c}$, therefore, will then be a maximum for the series. The spectra for $\Theta = 150°$ and 180° are not shown, for they are the same as those for 60° and 30° respectively. The intensity of the 3650 cm^{-1} band is a maximum when $\Theta = 90°$, and decreases symmetrically as Θ changes from 90° to 0°, or from 90° to 180°.

The intensity and strongly directional character of the 3650 cm^{-1} band are further emphasized by a comparison of the spectra with polarized and unpolarized radiation for the same orientation of the sample. As would be expected, the intensity of this band relative to the others is much greater in the polarized spectrum for $\Theta = 90$ in Fig. 11 than it is for the unpolarized spectrum in Fig. 9 ($\varphi = 20°$). With the beam unpolarized, the

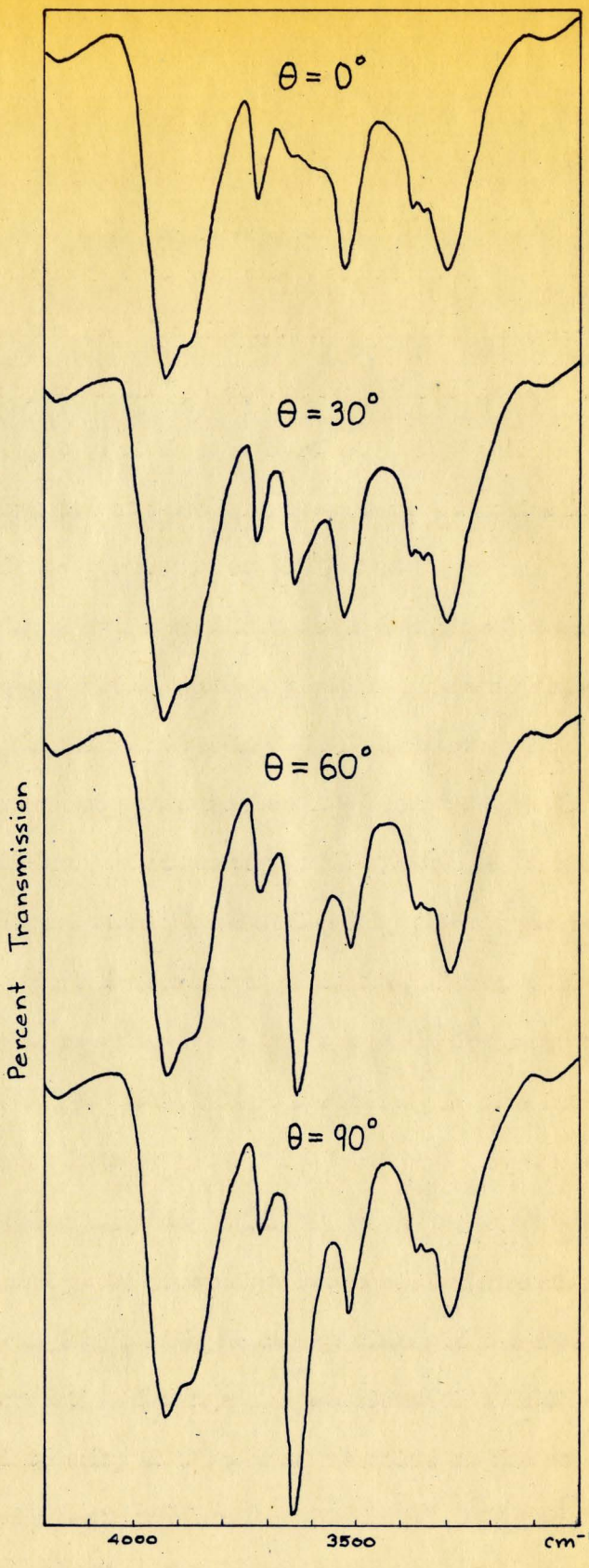

Fig. 11. Infrared Spectra of Portlandite with $\varphi = 20°$, Polarized Radiation, and Various Values of θ

isotropic vibrations and the 3650 cm^{-1} vibration each absorb a certain proportion of the incident radiation. When the beam is polarized and the electric vector of the radiation lies in the direction in which the 3650 cm^{-1} vibration is most sensitive, the isotropic vibrations still absorb the same proportion of the incident light, but the 3650 cm^{-1} vibration absorbs a much greater proportion than before, and hence is relatively much stronger.

3.3 Spectra Obtained with the Liquid Helium Apparatus and Unpolarized Radiation.

This work, as previously mentioned, was done at the MacLennan Laboratory, University of Toronto, using a Perkin-Elmer Model 12C single-beam spectrometer equipped with a 60° LiF prism.

Fig. 12 shows a background spectrum (#1) and a series of portlandite spectra, over the range 4600-3000 cm^{-1}, obtained at various temperatures with φ approximately equal to 30°. Spectrum #1 shows that the atmospheric bands were not entirely removed by flushing the optical path with dry nitrogen gas. The intensity of the atmospheric absorption, however, was reduced sufficiently to prevent it from obscuring the features of the portlandite spectrum.

The main object of this study was to examine the spectrum at very low temperatures, but in order to observe the spectral changes as the temperature was falling, spectra were obtained during the slow cooling period after the liquid helium had been added to the cryostat. Some of these spectra are shown in Fig. 12. The temperature changed considerably while each of the spectra was being recorded, and only approximate mean temperatures with limits of variation can be given for them. The temperatures at which the illustrated spectra were recorded were as follows:

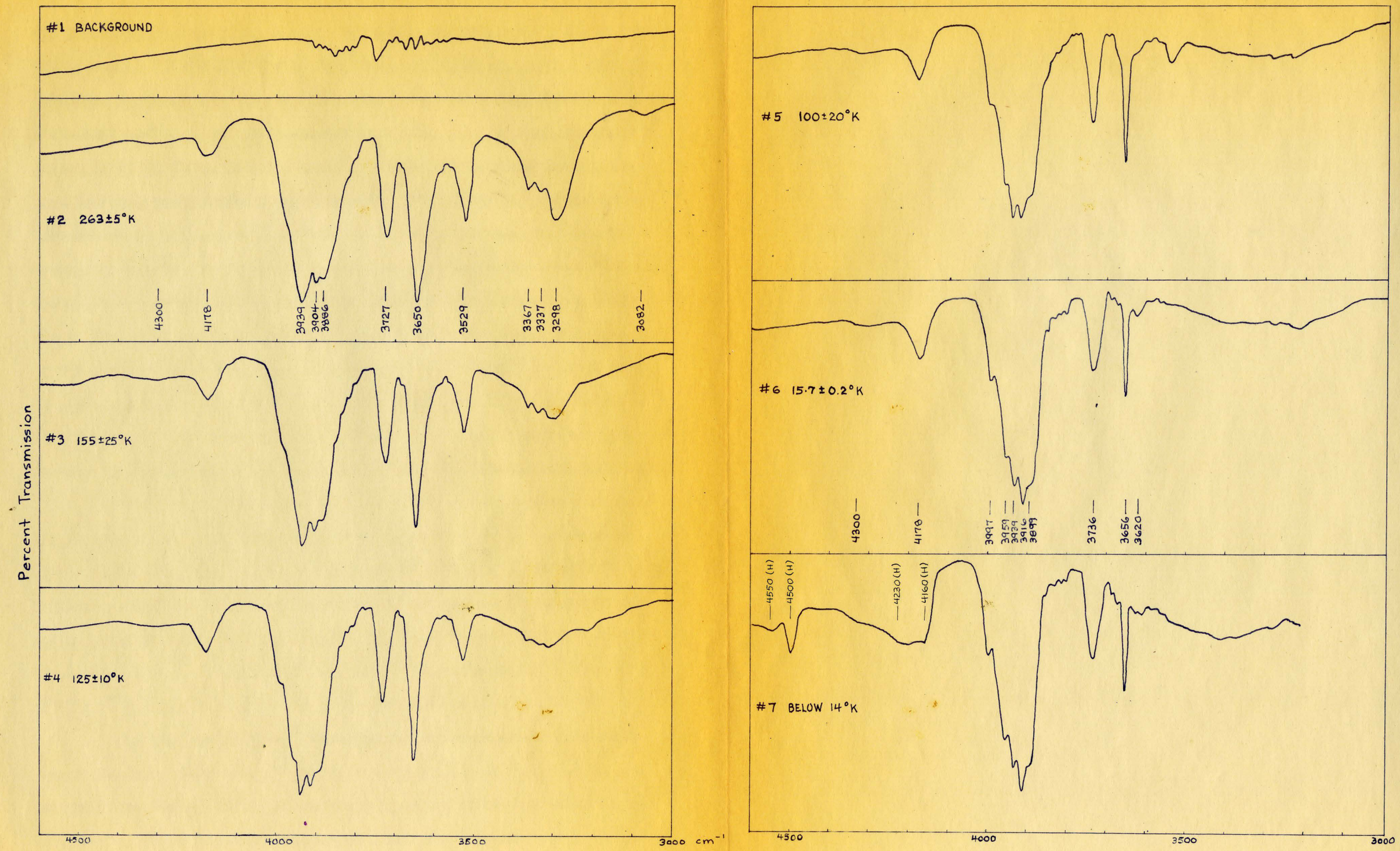

Fig. 12. Infrared Spectra of Portlandite at Various Temperatures, with φ Approximately 30° (Unpolarized Radiation)

#2, 263±5°K; #3, 155±25°K; #4, 125±10°K; #5, 100±20°K; #6, 15.7±0.2°K; #7, between 14°K and 4°K, the melting point of hydrogen and the boiling point of helium respectively. There are several changes in the broad band in the 4000-3800 cm^{-1} region. In spectrum #2 of Fig. 12, the band has three peaks, at 3939, 3904, and 3886 cm^{-1}. As the temperature drops, the band becomes more intense and narrower. Two shoulders appear on the high frequency side at 3997 and 3959 cm^{-1}, while the peak at 3886 cm^{-1} nearly disappears, becoming merely a shoulder centred at about 3899 cm^{-1}. Except for some narrowing, there seems to be little change in the 3939 cm^{-1} band. The 3904 cm^{-1} band appears to shift gradually to higher frequencies as the temperature decreases; the frequency is 3916 cm^{-1} by the time the temperature has fallen to 125°K, and increases little, if any, after that. This band becomes more and more prominent as the temperature drops until, at very low temperatures, it is considerably more intense than the others.

The 3727 cm^{-1} band becomes less intense as the temperature of the sample decreases. There is also an apparent shift in the frequency of the band to 3736 cm^{-1}, but this shift is very likely due, at least in part, to the strong atmospheric band at 3750 cm^{-1}, which becomes relatively stronger as the other weakens. In the recorded spectra the two bands are unresolved and, as a result, there is an apparent frequency shift in the 3727 cm^{-1} portlandite band as it decreases in intensity.

The band at 3650 cm^{-1} becomes much narrower; its half-width decreases from about 60 cm^{-1} at 263°K to about 15 cm^{-1} at 15.7°K. It also shows a gradual frequency shift. At temperatures below 125°K the frequency appears to remain constant at 3656 cm^{-1}. In addition to spectrum #6, two other spectra were obtained

appeared to be a positive frequency shift in some of the bands before they disappeared.

Some marked changes were observed in the 4600-4100 cm^{-1} region of the spectrum when the temperature of the sample was below 14°K, as shown in spectrum #7 of Fig. 12. A fairly strong band has appeared at about 4500 cm^{-1}, and a much weaker one at approximately 4550 cm^{-1}. In addition, the 4178 cm^{-1} band, which had gradually increased in intensity as the temperature decreased to 15.7°K, appears to have shifted to a slightly lower frequency and to have broadened out considerably on the high frequency side in the spectrum obtained at the temperature lower than 14°K. We believe that the explanation of these phenomena can be found in terms of the infrared absorption of solid and liquid hydrogen. Allin, Hare, and MacDonald (17) found a series of bands in this region. The approximate positions and frequencies of these bands are indicated above spectrum #7, and identified with the symbol (H). The frequency values, 4550, 4500, 4230, and 4160 cm^{-1}, were obtained from the figure given by Allin et al. The positions of these bands appear to correspond very well with those of the new features in spectrum #7; two of them coincide with the positions of the new bands at 4550 and 4500 cm^{-1}, and the others correspond to the extent of the apparent broadening on the high frequency side and shift to lower frequency of the 4178 cm^{-1} band. It will be remembered, that hydrogen gas had been introduced into the sample cell to conduct heat from the crystals to the cell walls. It is very probable, therefore, that the changes in the spectrum when the temperature of the sample was reduced below the melting point of hydrogen are due to the presence of solid hydrogen in the cell. Possibly some of the vapour

solidified on the crystal faces and on the interior surfaces of the cell windows.

Finally a rather broad band centred at about 4320 cm^{-1} can be seen in the spectra of Fig. 12. This band is very weak, however, and possibly not significant in the spectrum. If there is any change at all in this band as the temperature of the sample falls, it is a slight increase in intensity.

The spectra obtained with the Model 12C spectrometer, as with the Model 21, were recorded in terms of percent transmission. In Fig. 13 are shown three of the spectra with percent transmission values ~~values~~ converted to absorption. The three absorption profiles, #1, 2, and 3, were derived from three spectra of Fig. 12: #2, 6, and 7 respectively. The approximate temperatures are, therefore, #1, 263°K; #2, 15.7°K; #3, between 14° and 4°K. The conversion from transmission to absorption values was done using the relationship,

$$I(\nu) = I_o(\nu)e^{-\alpha(\nu)x},$$

where $I(\nu)$ is the intensity of the transmitted radiation, $I_o(\nu)$ the intensity of the incident radiation, $\alpha(\nu)$ the absorption coefficient, and x the thickness of the sample. From this expression it can be seen that $\alpha(\nu)$, the absorption coefficient, is proportional to $\log (I_o/I)$, where the logarithm is taken either to the base e or to the base ten.

The value of $\log_{10}(I_o/I)$ was found in the following manner. First a copy of the background spectrum was traced on the chart containing the portlandite spectrum. The vertical position of the background spectrum relative to the other was chosen by matching it with the portlandite spectrum at positions where it appeared that transmission by the portlandite sample

Fig. 13. Infrared Absorption Profiles of Portlandite at Various Temperatures ($\varphi = 30°$, and Radiation Unpolarized)

would have been one hundred percent had it not been for scattering and reflection by the sample and cell windows. The base line for all measurements was found by closing off the beam and observing the position of the pen for zero transmission. At intervals of 5 cm^{-1} in regions where there were atmospheric bands, and 10 or 20 cm^{-1} elsewhere, values proportional to I_o and I were found by measuring the vertical distances from the base line to the background spectrum and to the portlandite spectrum respectively. These values were converted to logarithms to the base ten, and the difference of each pair with the same ordinate found to give the value of $\log_{10}(I_o/I)$. This quantity was then plotted as a function of wavenumber to give the absorption profiles shown in Fig. 13.

The region from 3000 to 2800 cm^{-1}, which was not shown in the previous spectra of the portlandite plates, is reproduced in Fig. 13. There are three bands in this region, at 2960, 2920, and 2850 cm^{-1}, the first a very weak one. These bands appeared in all of the spectra of the composite section of portlandite plates. They showed no polarization properties, and appeared unchanged throughout the temperature range over which the sample was studied. Nujol has two extremely intense absorption bands at about 2920 and 2850 cm^{-1}, and the bands appearing in the portlandite spectrum at these frequencies were, in all likelihood, due to traces of nujol. In early infrared studies with the thin crystal sections, they had been placed on a CaF_2 plate and held there with nujol. An attempt had been made to clean the crystals with various organic solvents, but traces of it must have remained on the sample. The source of the weak band at 2960 cm^{-1} is not certain, but it may be due to one of the solvents used;

several organic compounds have strong absorption bands in this region. It is almost certain, at any rate, that the three bands in the region between 3000 and 2800 cm^{-1} are not due to absorption in portlandite, for they do not appear in the spectrum of the powdered sample (Fig. 8); this sample was prepared from fragments of portlandite which had not been in contact with nujol.

In Fig. 14 the absorption profiles are superimposed in order that they may be compared more easily. In Fig. 14 (a), the spectrum obtained at 15.7°K is superimposed on the spectrum obtained at 263°K. The changes in the spectrum with temperature, which were discussed earlier, are shown very clearly in this figure. It appears that the frequency shift in the 3727 cm^{-1} band is not due entirely to the presence of the atmospheric band at 3750 cm^{-1}, for a shift is apparent in this figure. It should be pointed out, however, that the atmospheric background did not subtract out completely when the absorption profiles were plotted, possibly because the flushing with dry nitrogen had been more efficient when the background trace was obtained than when these particular portlandite spectra were recorded. Comparison of the two profiles also reveals that the weak band which seemed to be centred at about 4320 cm^{-1} does increase in intensity as the temperature falls. In the absorption profiles, however, it appears as a plateau or broad shoulder on the side of the 4178 cm^{-1} band. It is difficult to assign any frequency value to this shoulder, but it appears to be centred closer to 4300 than to 4320 cm^{-1}.

Fig. 14 (b) shows the spectrum obtained at a temperature below 14°K superimposed on the one obtained at 15.7°K. Only a few changes

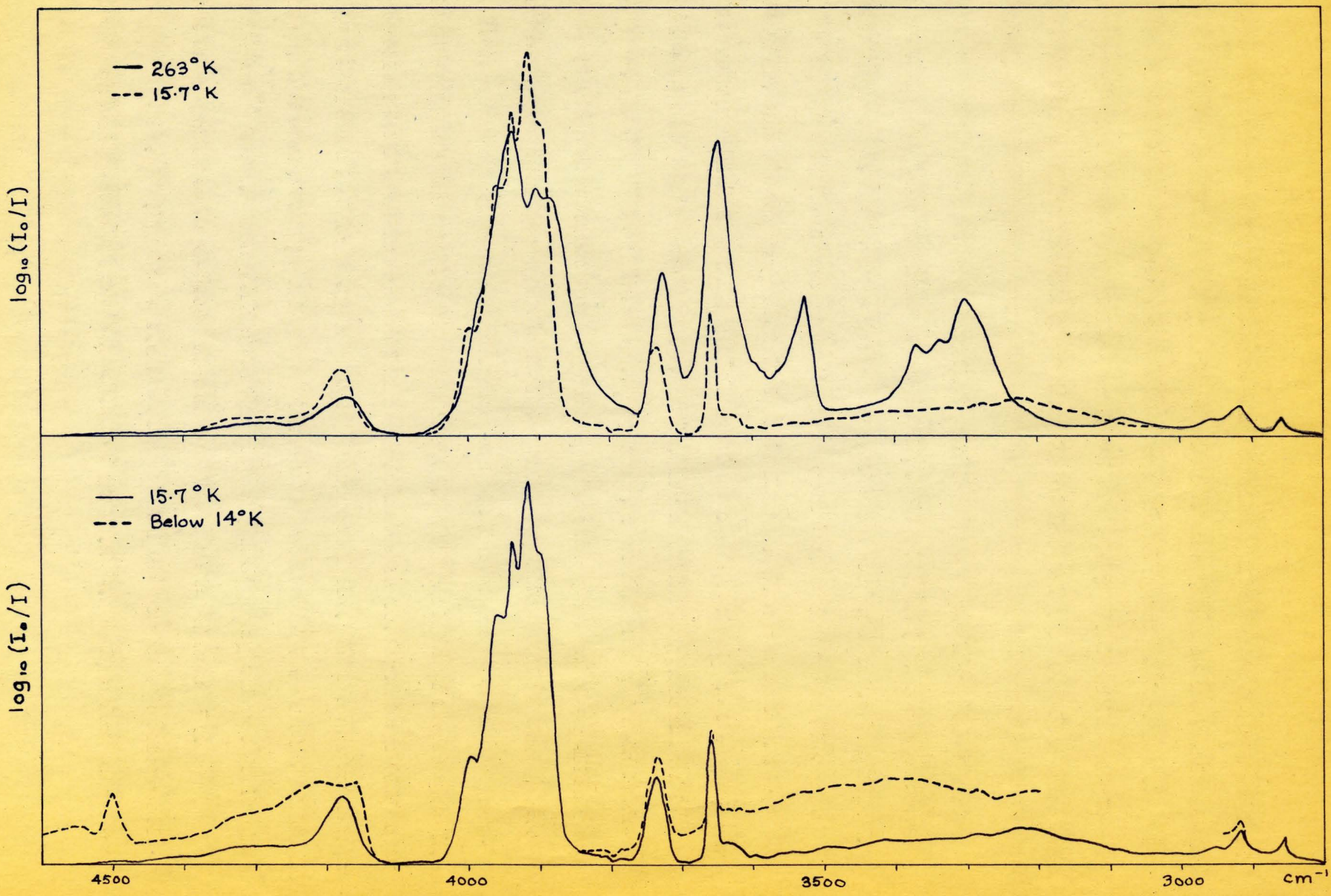

Fig. 14. Comparison of Absorption Profiles for Various Temperatures of the Sample ($\varphi = 30°$, and Unpolarized Radiation)

are evident. Those on the high frequency side of the broad, intense band have already been discussed. In addition, there seems to be a marked, overall increase in absorption between 3800 and 2800 cm^{-1}. This increase may be the result of a slight change in the physical properties of the sample which affected the scattering characteristics, but is more probably due simply to the presence of solid hydrogen, causing either increased absorption or more scattering in this region.

The spectroscopic equipment in the MacLennan Laboratory had certain advantages over the Model 21 spectrometer. A LiF prism has somewhat higher resolving power than a CaF_2 prism, and hence the fine structure in the broad bands was resolved more clearly with the Model 12C spectrometer. Moreover, the spectra were recorded with a longer wavenumber scale, making it easier to determine the frequency of the bands. This was especially true in the region above 4000 cm^{-1}, in which the wavenumber scale in the Model 21, with the CaF_2 prism installed, was compressed by a factor of ten. The greatest advantage lay in the optical set-up, with the exterior rock salt lenses. With them the optical beam could be focused almost entirely on the sample, thus giving a much stronger signal at the detector than was possible with the Model 21 and, as a result, a higher signal-to-noise ratio. All these factors combined to make the results obtained with the Model 12C somewhat more reliable than those obtained with the Model 21; hence they were used for obtaining the frequencies of most of the bands in the spectrum. Because a spectrum at room temperature was not obtained with the Model 12C spectrometer, the bands are identified by their frequencies at 263°K rather than at room temperature.

3.4 Spectra Obtained at Low Temperature with the Model 21 Spectrometer

For these spectra the composite section of thin plates was mounted in the cold cell illustrated in Fig. 4. Several spectra were obtained with polarized radiation. For these, liquid air was used as the coolant; with it the temperature of the sample varied between 105°and 115°K, which is within the temperature range over which spectrum #5 of Fig.12 was recorded. The sample was orientated with $\varphi = 0°$ and $30°$, and for each of these settings, spectra were obtained with $\theta = 0°$, $30°$, $60°$, and $90°$. The complete polarization of the 3650 cm^{-1} band was again demonstrated, but no further polarization properties were detected in the spectrum over the frequency range studied (4600-2800 cm^{-1}).

Megaw (17) in her X-ray work on portlandite, found a discontinuous change of spacing, 0.07 percent in magnitude, perpendicular to the triad axis at a temperature just above the boiling point of nitrogen. There is a possibility that the discontinuity is reflected in the behaviour of the infrared spectrum, but nothing of this sort was observed in the spectra obtained with the liquid helium apparatus. If the discontinuity in the behaviour of the spectrum is small, however, it could easily have been missed because of the large difference between the temperatures at which the various spectra of Fig. 12 were recorded. An attempt to discover a discontinuity was made with unpolarized radiation and a crystal orientation of $\varphi = 20°$, using the Model 21 spectrometer. Liquid nitrogen was used as the coolant, and the temperature of the sample was lowered as much as possible by pumping on the chamber containing the liquid nitrogen with a vacuum pump of fairly high capacity. The lowest temperature attained was 86°K, nine degrees higher

than the boiling point of nitrogen. Between 115°K and this temperature there did not appear to be a discontinuity in the spectral range studied, 4600-2800 cm^{-1}. The increase in intensity of the band at 3916 cm^{-1} is fairly rapid, however, and it is possible that above 86°K there is a slight discontinuity in the change in this band with temperature which was not detected. It can be stated with reasonable certainty, though, that if the discontinuous change in spacing observed by Megaw does result in a discontinuity in the change of infrared absorption with temperature between 4600 and 2800 cm^{-1}, the discontinuity is fairly small, and probably occurs below 86°K.

The low temperature results obtained with the Model 21 spectrometer were useful in checking some of the frequency values observed with the Model 12C and the liquid helium apparatus. As mentioned previously, a spectrum was not obtained at room temperature with the latter equipment, and hence the bands of the spectrum of portlandite were identified by their frequency values at 263°K. With the Model 21 there was poorer resolution, and the frequency shifts occurring in the complex band between 4000 and 3800 cm^{-1} could not be determined with certainty. The shift in the frequency of the 3650 cm^{-1} band between room temperature and 110°K, however, was found to be about 6 cm^{-1}. Approximately the same frequency change was observed between 263° and 110°K in the spectra obtained with the Model 12C. The indication, therefore, is that the change in the frequencies of the bands between room temperature and 263°K is not great, and that the frequencies of the bands with the sample at 263°K are close to the values for room temperature.

With the Model 21 the frequency shift in the 3726 cm^{-1} band between room temperature and liquid air temperatures was found to be approximately 5 cm^{-1}. Although the atmospheric compensation with the double-beam instrument was not perfect with the low temperature cell and the compensating cell in the spectrometer beams, the atmospheric band at 3750 cm^{-1} did not remain with sufficient intensity to account for so great a change. It seems, then, that only a part of the shift observed in the 3726 cm^{-1} band in the spectra obtained with the Model 12C spectrometer is due to the presence of the atmospheric band. There appears to be a real frequency shift of a few wavenumbers as well.

3.5 The Infrared Spectrum of Brucite

The infrared absorption of brucite was studied briefly for decreasing temperature of the sample, and the behaviour of the bands was found to parallel very closely that of the equivalent bands in the portlandite spectrum. Three spectra over the range 4500-3000 cm^{-1}, obtained with unpolarized radiation and $\varphi = 20°$, are shown in Fig. 15. The approximate temperatures of the sample when each of these spectra was recorded were: #1, 293°K (room temperature); #2, 202°K; #3, 105°K. The two lower temperatures were achieved by mounting the sample in the cold cell and using as the coolant a mixture of crushed dry ice and acetone for the first, and liquid air for the second. The frequency values of the bands in the spectrum of brucite were determined only approximately, and are given here to roughly three-figure accuracy.

The broad band in the spectrum between 4100 and 3900 cm^{-1} corresponds to the broad band in the 4000-3800 cm^{-1} region in the spectrum

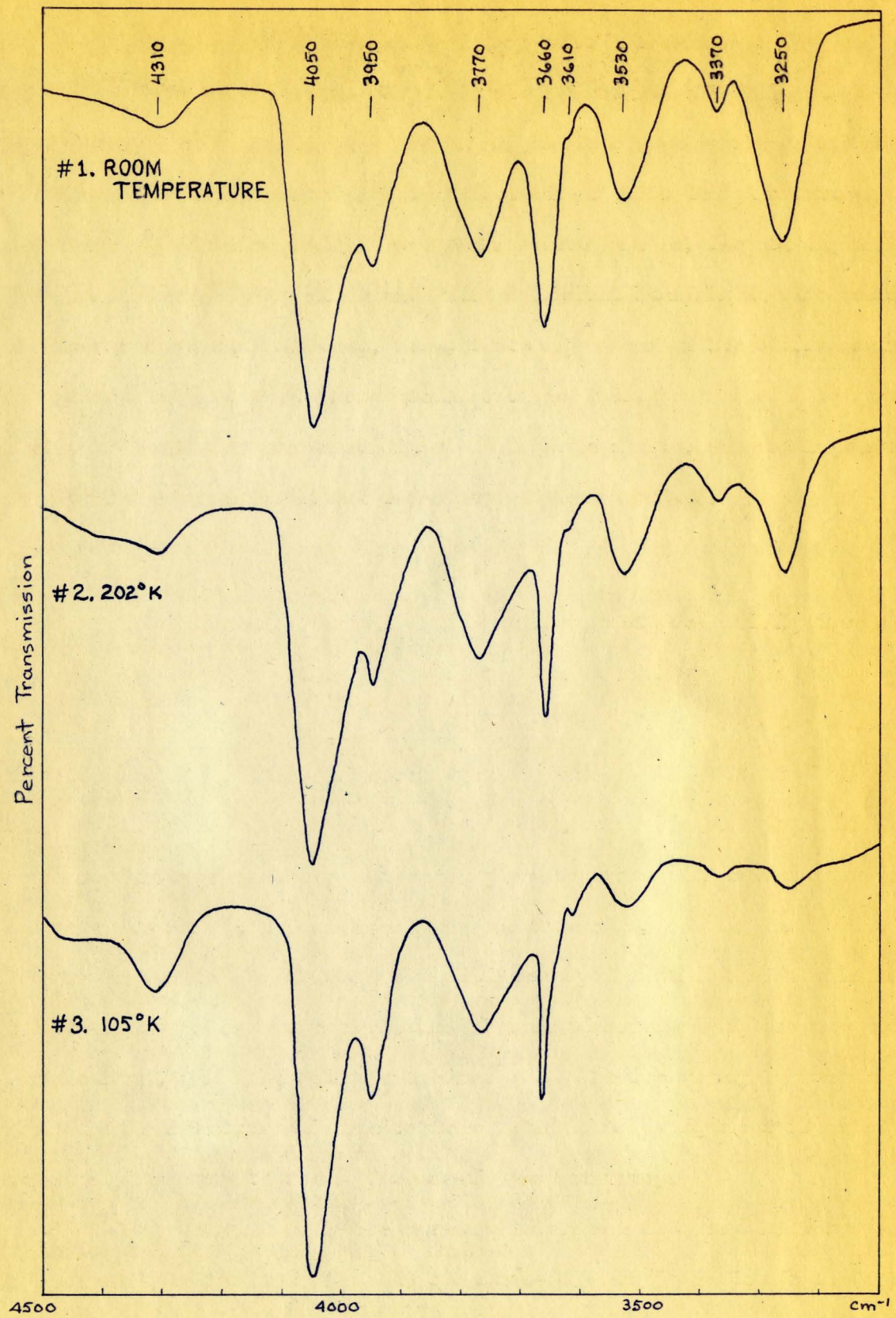

Fig. 15. Infrared Spectra of Brucite with $\varphi = 20°$, Unpolarized Radiation, and the Sample at Various Temperatures

of portlandite. In this series, however, all of the fine structure of the band is not resolved because a portion falls in the region above 4000 cm^{-1}, where the wavenumber scale is compressed by a factor of ten with the Model 21 spectrometer when the CaF_2 prism is installed. The general behaviour of the band, though, is seen to be similar to that of the broad band in the spectrum of portlandite. As the temperature of the sample decreases, the band becomes more intense and somewhat narrower, and the fine structure becomes more sharply resolved.

The narrow band at 3660 cm^{-1} corresponds to the polarized band at 3650 cm^{-1} in portlandite, when $\varphi=0^{\circ}$, its intensity is a minimum, and as φ increases; the intensity greatly increases. The low temperature behaviour also corresponds to that of the equivalent band in portlandite. As the temperature falls, the band becomes considerably narrower, decreases in intensity, and appears to shift to a slightly higher frequency. There is also a shoulder, on the low frequency side of the band, which becomes better resolved as the 3660 cm^{-1} band narrows. The appearance of this shoulder tends to confirm the presence of the similar shoulder in portlandite. Unfortunately, its polarization properties were not tested.

The behaviour of the other bands in the spectrum is also similar to that of the corresponding bands in the spectrum of portlandite. The 4310 cm^{-1} band becomes more intense as the temperature decreases. The 3770 cm^{-1} band decreases in intensity, and shows a small positive frequency shift. The bands below 3600 cm^{-1} decrease very considerably in intensity, and are very weak when the temperature of the sample has fallen to 105°K.

The infrared spectrum of brucite was not considered in great enough detail to permit saying that it is entirely equivalent to the spectrum of portlandite. From this work, however, it is apparent that the similarities are very marked, and appear to hold throughout the temperature range over which the brucite was studied. Certainly as far as general appearance and temperature dependence are concerned, there appears to be no discrepancy between the spectra of the two substances.

3.6 Discussion

In the table on the following page are listed the absorption bands detected in the infrared spectrum of portlandite in the spectral region 4600-2800 cm^{-1}, with the temperature of the sample ranging from room temperature to below 14°K, the freezing point of hydrogen. The first three temperatures given in the table, 263°, 125°, and 15.7°K, are the approximate mean values of the temperature ranges over which spectra #2, 4, and 6 of Fig. 12 were recorded, and "below 14°K" represents the temperature region of the sample when spectrum #7 was recorded. The frequencies of the bands appearing in each spectrum are listed under the corresponding temperature value. When a band was not detected at a particular temperature, no frequency value is given for the band in that column. The total frequency shifts observed and the intensity changes are also tabulated. Except for the low temperature frequencies of the 3727 cm^{-1} band, all frequency values given are those obtained with the Model 12C spectrometer.

Table of the Infrared Absorption Bands

Detected in Portlandite Between 4600 and 2800 cm^{-1}

Frequencies (in cm^{-1}) of the Infrared Bands in Portlandite at:				Total Frequency Shift (cm^{-1})	Change in Intensity
263 K	125 K	15.7 K	Below 14 K		
4300	4300	4300	4300		Increase
4178	4178	4178	4178		Increase
--	3997	3997	3997		Increase
--	3959	3959	3959		Increase
3939	3939	3939	3939		
3904	3916	3916	3916	+12	Increase
3886	3899	3899	3899	+13	Decrease
3727	3732	3732	3732	+5	Decrease
3650	3656	3656	3656	+6	Decrease
--	--	3620	3620		Unknown
3529	3529	--	--		Decrease
3367	3369	--	--		Decrease
3337	3339	--	--		Decrease
3298	3310	--	--		Decrease
3082	--	--	--		Decrease

Although a frequency shift seems to occur in some of the bands on the low frequency side of the 3650 cm^{-1} band, no values are given for the shifts because of the uncertainty of their extent before the bands disappeared. A value of 5 cm^{-1} is given for the frequency shift in the 3727 cm^{-1} band. This is the change observed with the double-beam Model 21 spectrometer, where the effect of the atmospheric band at 3750 cm^{-1} was small. Using the value of 5 cm^{-1} for the shift makes the final low temperature value of the frequency of the band 3732 cm^{-1}, rather than 3736 cm^{-1} as obtained with the Model 12C.

The band at 3650 cm^{-1}, and possibly the shoulder at 3620 cm^{-1}, were the only ones which revealed any polarization properties; the 3650 cm^{-1} band showed complete polarization, with the direction of polarization parallel to the c axis. It is difficult to say whether the intensity is actually zero when φ is equal to zero, that is, when the $\underline{E}$ vector is perpendicular to the c axis. The experimental results indicated, though, that the value is very close to zero. The vibration leading to the 3650 cm^{-1} band, therefore, must have a very small component perpendicular to the c axis; in other words, the motion must take place essentially in a direction parallel to c.

None of the other bands which were detected revealed any polarization properties. If the spectra of brucite and portlandite are equivalent, this result appears to contradict the findings of Mara and Sutherland (6), who observed that several of the bands in this region of the spectrum of brucite possess some polarization properties. It may well be, however, that some of the bands in the portlandite spectrum are

polarized, and that these properties were not detected. Because of the small size of the sample and the considerable reduction of intensity when the polarizer was in the beam, the intensity of the radiation at the detector was very low when the spectra with polarized radiation were recorded. As a result, the resolution of the bands was poor, and became worse as φ increased and the effective sample width became smaller. The maximum value of φ for which the spectrum was studied with polarized radiation was 40°, and even with this orientation, resolution was too poor to reveal any small changes which might have occurred in the bands as the $\underline{E}$ vector was rotated. As φ was made larger than 40°, the definition of the peaks in the spectrum rapidly fell off. In order to obtain conclusive results about polarization properties, a thin plate of portlandite cut perpendicular to the cleavage plane would be very useful. In such a sample, the $\underline{c}$ axis would lie in the plane of the crystal plate, and spectra with polarized radiation could be obtained for $\underline{E}$ both perpendicular and parallel to the $\underline{c}$ axis. The latter orientation would permit determining with certainty if any of the bands in the spectrum are completely or partially polarized in the plane perpendicular to $\underline{c}$ because such bands would either be absent or show greatly reduced intensity.

Busing and Levy (18) have located the protons in portlandite by neutron diffraction, and their findings confirm the direction for the O-H bond indicated by the X-ray study of Petch (12). Any explanation of the mechanism leading to the infrared absorption must be made, therefore, in terms of the Bernal-Megaw model of the crystal structure with the O-H bond parallel to the $\underline{c}$ axis of the crystal.

The band at 3650 cm^{-1} (2.74μ) has the polarization properties and frequency expected of the fundamental OH-stretching vibration. If, as Hexter and Dows (11) have suggested, the complex absorption pattern results from the coupling of the fundamental vibration with a librational motion of the ion, the 3650 cm^{-1} band should be accompanied by low and high frequency combination bands. The low frequency bands would result from transitions involving excited librational levels, and their intensity should decrease on cooling, while the high frequency bands, originating in the ground state, should increase in intensity at low temperatures. The spectra which were obtained are in qualitative agreement with this model. All the bands below the polarized band at 3650 cm^{-1} decreased in intensity as the temperature of the sample was lowered, and most of the bands above increased in intensity. There were discrepancies, however; the intensity of the 3727 cm^{-1} band, rather than increasing as would be expected, decreased as the temperature was lowered. Some of the bands, notably that in the 4000-3800 cm^{-1} region, possess fine structure which is not explained by the simple model described above.

No attempt will be made here to interpret the complex pattern of the infrared absorption. The main purpose of this work was to examine carefully the infrared absorption of a single crystal of portlandite and to report any findings. Unfortunately, for reasons given, the study of the polarization properties of the bands in the spectrum was inadequate. It is hoped, however, that the results will prove helpful, those obtained at very low temperatures in particular, in solving the complicated pattern which exists in the infrared spectrum of portlandite in the region of the fundamental OH-stretching band.

BIBLIOGRAPHY

(1) C. E. Tilley, Min. Mag. 23, 419, (1933)

(2) F. W. Ashton and R. Wilson, Am. J. Sc. 13, 209, (1927)

(3) H.D.Megaw, Proc. Roy. Soc. (London) A142, 198, (1933)

(4) G. Aminoff, Geol. Foren. i Stockholm Forh. 41,407, (1919)

(5) J.D.Bernal and H.D.Megaw, Proc. Roy. Soc. (London) A151, 384, (1935)

(6) R.T.Mara and G.B.B.M. Sutherland, J. Opt. Soc. Am. 43, 1100, (1953)

(7) H. E. Petch and H.D.Megaw, J. Opt. Soc. Am. 44, 744, (1954)

(8) H. E. Petch, Phys. Rev. 99, 1635, (1955)

(9) D.D.Elleman and D. Williams, J.Chem. Phys. 25, 742, (1956)

(10) R.T. Mara and G.B.B.M. Sutherland, J.Opt. Soc. Am. 46, 464, (1956)

(11) R.M.Hexter and D.A.Dows, J. Chem. Phys. 25, 504, (1956)

(12) H.E.Petch, Can. J. Phys. 35, 983, (1957)

(13) H.W.Woolley, R.B.Scott, and G.G.Brickwedde, J.Res.N.B.S. 41, 379, (1948).

(14) J.G.Aston, Temperature, Its Measurement and Control in Science and Industry, Reinhold Publishing Corporation, New York, 219, (1941)

(15) W.P.Wood and J.M. Cork, Pyrometry, McGraw-Hill Book Company, New York, (1927)

(16) R.B.Scott, Temperature, Its Measurement and Control in Science and Industry, Reinhold Publishing Corporation, New York, 206, (1941)

(17) H.D.Megaw, International Conference on Current Problems in Crystal Physics, Preprints of Papers, Massachusetts Institute of Technology, 38, (1957)

(18) W. R. Busing and H. A. Levy, J. Chem. Phys. 26, 563, (1957)